ISSN 2176-5480

22nd International Congress of Mechanical Engineering (COBEM 2013)
November 3-7, 2013, Ribeirão Preto, SP, Brazil

APPLICATION OF MODEL-BASED PREDICTIVE CONTROL APPROACHES IN A THREE-PHASE INDUCTION MOTOR

Eduardo Bonci Cavalca
José de Oliveira
Mariana Santos Matos Cavalca
Ademir Nied
UDESC - Universidade do Estado de Santa Catarina, Joinville-SC, Brazil
e.cavalca@gmail.com, dee2jo@joinville.udesc.br, mcavalca@joinville.udesc.br, nied@joinville.udesc.br

Abstract. *Model-based predictive control (MPC) approaches has been studied in a wide range of areas, as petrochemical and aerospace, mainly due to its capability of easily dealing with physical and operational constraints. Moreover, such approaches can be extended for the application in control loops with nonlinear and time-variant systems. At this context, the objective of this work is to study some MPC techniques in order to evaluate their applicability to control a three-phase induction motor (TIM). More specifically, it was analyzed a Dynamic matrix control (DMC) approach, as well as a MPC technique that uses state space modeling. The control algorithms in question, as well as the nonlinear mathematical model of the motor in study, were programmed using the free computing environment Scilab-Xcos®. The TIM linear model used in MPC loop was obtained by a system identification method with are based on the step response of the classical non-linear model of a TIM. Multiple simulations have been performed considering variations in load and speed reference. Besides, some discussions are made in relation to the influence of the control parameters and about the computational cost. Simulation results demonstrate satisfactorily the characteristics of the proposed TIM control loop scheme.*

Keywords: *model-based predictive control, three-phase induction motor, system identification.*

1. INTRODUCTION

Model-based predictive control approaches were initially developed for applications in petrochemical industry, in which the time constants of the controlled processes are in order of hours (Qin and Badgwell, 2003; Lee, 2011). The first developments in the area date back to the 70's, but there are records of the application of its fundamental concepts in oil refineries in the 50's (Lee, 2011). Due to the MPC high computational cost, initially its application was not widespread

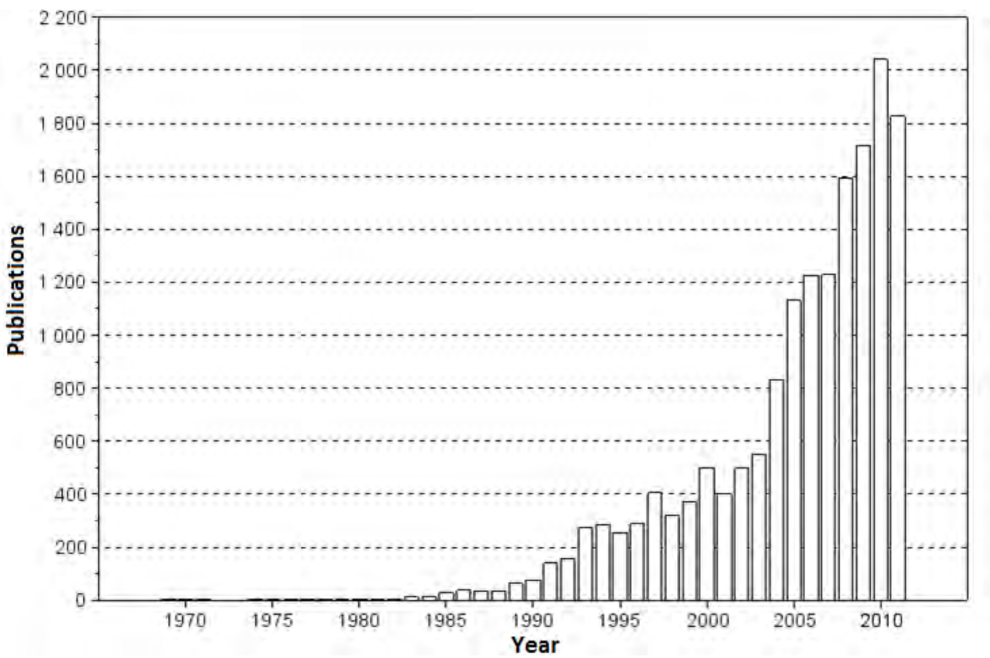

Figure 1. Evolution of the number of publications per year involving MPC approaches in Compedex® database. Search parameters - search for: predictive control; fields: subject, title and abstract; search date: August 10, 2012; search system: http://www.engineeringvillage.com.

ISSN 2176-5480

in systems with fast dynamics. However, as result of the technological advances over the years, nowadays such situation has been changing. A search conducted in Compendex® database showed that the number of publications per year in MPC area has grown significantly over the years, as shown in Fig. 1. This fact indicates that MPC approaches have been applied in a large number of differents systems, in which are among those with faster dynamic, as is the case of TIM (de Santana *et al.*, 2008).

At this context, this paper analyzes some MPC techniques, DMC and a State Space MPC (SSMPC) (Camacho and Bordons, 1999; Maciejowski, 2002; Rossiter, 2004), in order to evaluate if those approache have interresting characteristics to be applied in a TIM control loop. The control algorithms in question, as well as the TIM nonlinear mathematical model, were programmed using the free computing environment Scilab-Xcos®. TIM linear model was obtained by a system identification method based on the step response of TIM non-linear model in a certain operational point.

The remainder of this paper is organized as follows. Section 2 reviews the design of two MPC approaches: DMC and SSMPC. Section 3 presents a TIM modeling. Section 4 presents a case study for a specific TIM. The results are evaluated through numerical simulations. Concluding remarks are presented in Section 6.

Throughout the text, $\boldsymbol{I}_i$ represents an $i \times i$ identity matrix, $\mathbf{0}_{i\times j}$ represents a matrix with i lines and j columns full fill with zeros, $\boldsymbol{diag}(n_1, n_2, ..., n_m)$ defines a $m \times m$ diagonal matrix with elements $n_1, n_2, ..., n_m$, the notation $(\cdot|k)$ is used in predictions with respect to time k, and the $*$ superscript indicates an optimal solution. For brevity of notation, only the upper triangular part of symmetric matrices is explicitly presented. The s and r index are related to the TIM stator and the rotor, respectively, as well as the a, b and c index are related with the phases A, B and C respectively.

2. MODEL-BASED PREDICTIVE CONTROL

There are several MPC techniques, that together compose a family of controllers characterized mainly by three fundamental concepts: the use of a prediction model, a control action based on the minimization of a cost function and the receding horizon (Camacho and Bordons, 1999). The prediction model is a representative mathematical model of the process. It is used to predict, given a predifined horizon N, the values of the controlled variable will potentially take in future moments. Interactively, a sequence of M control actions is determined in order to minimize a cost function J. This cost function is usually defined to penalize tracking errors and control actions efforts. Only the first value of the optimal control sequence is applied, according to the concept of receding horizon (Camacho and Bordons, 1999; Maciejowski, 2002; Rossiter, 2004). This strategy allows the controller to re-evaluate the optimal control sequence in each sampling cycle based on feedback signals.

In general, MPC has the following main advantages (Camacho and Bordons, 1999; Maciejowski, 2002): works with systems with multiple inputs and outputs (MIMO) as a simple matricial expansion of the single input and single output (SISO) systems formulation; considers limitations of the actuators system and other process constraints; allows the use of the actuators near its limits; compensates measurement disturbances intrinsically. In contrast, predictive controllers have a high computational cost as compared to other classical control methods.

2.1 Dynamic matrix control

Dynamic matrix control, is one of the first developed MPC techniques. Such method uses a quadratic cost function, which penalizes both the tracking errors as the control efforts variations, weighted by μ and ρ, respectively. As a prediction model, DMC employs the unit step response of the system. Such fact is one of its main advantages, since it is simpler and faster than phenomenological modeling. However, in this point also lies one of its fundamental limitations: DMC is not applicable in unstable open loop systems.

Consider a MIMO system with $\boldsymbol{y}(k) \in \Re^q$, $\boldsymbol{u}(k) \in \Re^p$, a possible unconstrained DMC algorithm, for a certain T_{st} sample time, can be defined as (Camacho and Bordons, 1999):

Preliminary steps

1. Obtain the step response $\boldsymbol{g}_{ij}(n), n = 1, ..., N_s$ for the variation of input u_i $(i = 1, \ldots, p)$ in the output y_j $(j = 1, \ldots, q)$, both from a predefined operational point. Note that N_s is a sufficient greater number of samples for the system to reach steady state. It is assumed that $\boldsymbol{g}_{ij}(0) = 0$ and $\boldsymbol{g}_{ij}(n) = \boldsymbol{g}_{ij}(N_s)$, $\forall n \geq N_s$ $(i = 1, \ldots, p$ and $j = 1, \ldots, q)$. Note that y_j detonates the jth output, as well u_i, the ith input.
2. Set the controller parameters: output $\mu_j \geq 0$ $(j = 1, \ldots, q)$ and input $\rho_i > 0$ $(i = 1, \ldots, p)$ weights, prediction horizon N and control horizon M. Consider yet only control horizon, such that $M < N$.

ISSN 2176-5480

Initialization

1. Assemble the auxiliaries system dynamics matrices $\boldsymbol{G}_{aux}(i)$ for $(i = 0, ..., N)$ as:

$$\boldsymbol{G}_{aux}(i) = \begin{bmatrix} \boldsymbol{g}_{11}(i) & \boldsymbol{g}_{12}(i) & \cdots & \boldsymbol{g}_{1p}(i) \\ \boldsymbol{g}_{21}(i) & \boldsymbol{g}_{22}(i) & \cdots & \boldsymbol{g}_{2p}(i) \\ \vdots & \vdots & \ddots & \vdots \\ \boldsymbol{g}_{q1}(i) & \boldsymbol{g}_{q2}(i) & \cdots & \boldsymbol{g}_{qp}(i) \end{bmatrix} \tag{1}$$

2. Assemble the system dynamics matrix $\boldsymbol{G}(i)$ as:

$$\boldsymbol{G} = \begin{bmatrix} \boldsymbol{G}_{aux}(1) & O_{q\times p} & \cdots & \boldsymbol{O}_{q\times p} \\ \boldsymbol{G}_{aux}(2) & \boldsymbol{G}_{aux}(1) & \cdots & \boldsymbol{O}_{q\times p} \\ \vdots & \vdots & \ddots & \vdots \\ \boldsymbol{G}_{aux}(N) & \boldsymbol{G}_{aux}(N-1)(i) & \cdots & \boldsymbol{G}_{aux}(N-M+1)(i) \end{bmatrix} \tag{2}$$

3. Assemble the weight matrices: $\boldsymbol{Q} = diag(\mu_1, \mu_2, \ldots, \mu_q)$ (size $q \times q$) and $\boldsymbol{R} = diag(\rho_1, \rho_2, \ldots, \rho_p)$ (size $p \times p$) .
4. Assemble the weight matrices: $\bar{\boldsymbol{Q}} = diag(\boldsymbol{Q}, \boldsymbol{Q}, \ldots, \boldsymbol{Q})$ (size $qN \times qN$) and $\bar{\boldsymbol{R}} = diag(\boldsymbol{R}, \boldsymbol{R}, \ldots, \boldsymbol{R})$ (size $pM \times pM$).
5. Determine controller gains matrix $\boldsymbol{K}_{DMC}$ as:

$$\boldsymbol{K}_{DMC} = \begin{bmatrix} \boldsymbol{I}_p & \boldsymbol{0}_{p\times p(M-1)} \end{bmatrix} \left(\boldsymbol{G}^T\bar{\boldsymbol{Q}}G + \bar{\boldsymbol{R}}\right)^{-1} \boldsymbol{G}^T\bar{\boldsymbol{Q}} \tag{3}$$

6. Let $k = 0$, $\Delta u_j(-i) = 0$ for $j = 0, ..., p$ and $i = 1, ...N_s$.

Main Routine

1. Read the process output $\boldsymbol{y}(k)$ and the reference $\boldsymbol{y}_{ref}(k) \in \Re^p$.
2. Determine the free-response vector $\boldsymbol{F}$ as:

$$\boldsymbol{F} = \begin{bmatrix} \boldsymbol{f}(k+1), \boldsymbol{f}(k+2), ..., \boldsymbol{f}(k+N) \end{bmatrix}^T \tag{4}$$

in which $\boldsymbol{f}(k+i) = \begin{bmatrix} f_1(k+i), f_2(k+i), ..., f_q(k+i) \end{bmatrix}^T$ and

$$f_j(k+i) = y_j(k) + \sum_{p}^{l=1} \sum_{N_s}^{n=1} \left\{ \left[\boldsymbol{g}_{jl}(n+i) - \boldsymbol{g}_{jl}(n)\right] \Delta u_l(k-n) \right\} \tag{5}$$

for $j = 1, 2, ..., q$ and $i = 1, 2, ..., N$.

3. Assemble the reference vector as $\boldsymbol{Y}_{ref} = [\boldsymbol{y}_{ref}, \boldsymbol{y}_{ref}, ..., \boldsymbol{y}_{ref}]$ (size $pN \times 1$).
4. Determine the control increment, give by

$$\boldsymbol{\Delta u}(k) = \boldsymbol{K}_{DMC}(\boldsymbol{Y}_{ref} - \boldsymbol{F}) \tag{6}$$

5. Update the control action making $\boldsymbol{u}(k) = \boldsymbol{u}(k-1) + \boldsymbol{\Delta u}(k)$.
6. Do $k = k + 1$, wait a sampling time and return to the first step of the main routine.

It is important to note that the preliminary and initialization parts of the control algorithm are made offline. The values of N and M, and weights ρ and μ, can be modified as needed by adjusting the desired behavior of the control loop. It is possible to note that larger values of N and M improve the transient behavior of the control loop, but increase the computational load. Finally, the weights ρ and μ ponder the intensity of the control signals to be applied.

2.2 State space model-based predictive control

State space MPC or SSMPC, as the name implies, uses a state space mathematical modeling to represent the process behavior. It is important to note that in order to employ the model in state space, first it is necessary to obtain a discrete-time representation for a determined sample time T_{st}. Consider a linear discrete-time representation around a certain operational of a MIMO process, with T_{st} sample time, of the form:

$$\boldsymbol{x}(k+1) = \boldsymbol{A}\boldsymbol{x}(k) + \boldsymbol{B}u(k) \tag{7}$$

$$\boldsymbol{y}(k) = \boldsymbol{C}\boldsymbol{x}(k) \tag{8}$$

where for each k, $\boldsymbol{x}(k) \in \Re^n$, $\boldsymbol{y}(k) \in \Re^q$, $\boldsymbol{u}(k) \in \Re^p$ and $\boldsymbol{A}$, $\boldsymbol{B}$ and $\boldsymbol{C}$ are matrices of appropriate dimensions.

A possible unconstrained SSMPC algorithm, for a certain T sample time, can be defined as (Maciejowski, 2002):

ISSN 2176-5480

Preliminary steps

1. Obtain the state space matrices $\boldsymbol{A}$, $\boldsymbol{B}$ and $\boldsymbol{C}$.
2. Set the controller parameters: output $\mu_j \geq 0$ $(j = 1, \ldots, q)$ and input $\rho_i > 0$ $(i = 1, \ldots, p)$ weights, prediction horizon N and control horizon M. Consider yet only control horizon, such that $M < N$.

Initialization

1. Assemble a extend state space model as:

$$\tilde{\boldsymbol{A}} = \begin{bmatrix} \boldsymbol{A} & \boldsymbol{0}_{n\times q} \\ \boldsymbol{CA} & \boldsymbol{I}_q \end{bmatrix}, \quad \tilde{\boldsymbol{B}} = \begin{bmatrix} \boldsymbol{B} \\ \boldsymbol{CB} \end{bmatrix}, \tilde{\boldsymbol{C}} = \begin{bmatrix} \boldsymbol{0}_{q\times n} & \boldsymbol{I}_q \end{bmatrix} \tag{9}$$

2. Assemble the system dynamics matrix $\boldsymbol{G}$ as:

$$\boldsymbol{G} = \begin{bmatrix} \tilde{\boldsymbol{C}}\tilde{\boldsymbol{B}} & \boldsymbol{0}_{q\times p} & \boldsymbol{0}_{q\times p} & \boldsymbol{0}_{q\times p} \\ \tilde{\boldsymbol{C}}\tilde{\boldsymbol{A}}\tilde{\boldsymbol{B}} & \tilde{\boldsymbol{C}}\tilde{\boldsymbol{B}} & O_{q\times p} & \boldsymbol{O}_{q\times p} \\ \vdots & \vdots & \ddots & \vdots \\ \tilde{\boldsymbol{C}}\tilde{\boldsymbol{A}}^{N-1}\tilde{\boldsymbol{B}} & \tilde{\boldsymbol{C}}\tilde{\boldsymbol{A}}^{N-2}\tilde{\boldsymbol{B}} & \ldots & \tilde{\boldsymbol{C}}\tilde{\boldsymbol{A}}^{N-M}\tilde{\boldsymbol{B}} \end{bmatrix} \tag{10}$$

3. Assemble the dynamic free-response matrix $\boldsymbol{\phi}$ as:

$$\boldsymbol{\phi} = \begin{bmatrix} \tilde{\boldsymbol{C}}\tilde{\boldsymbol{A}} \\ \tilde{\boldsymbol{C}}\tilde{\boldsymbol{A}}^2 \\ \vdots \\ \tilde{\boldsymbol{C}}\tilde{\boldsymbol{A}}^N \end{bmatrix} \tag{11}$$

4. Assemble the weight matrices: $\boldsymbol{Q} = diag(\mu_1, \mu_2, \ldots, \mu_q)$ (size $q \times q$) and $\boldsymbol{R} = diag(\rho_1, \rho_2, \ldots, \rho_p)$ (size $p \times p$).
5. Assemble the weight matrices: $\bar{\boldsymbol{Q}} = diag(\boldsymbol{Q}, \boldsymbol{Q}, \ldots, \boldsymbol{Q})$ (size $qN \times qN$) and $\bar{\boldsymbol{R}} = diag(\boldsymbol{R}, \boldsymbol{R}, \ldots, \boldsymbol{R})$ (size $pM \times pM$).
6. Determine controller gains matrix $\boldsymbol{K}_{SSMPC}$ as:

$$\boldsymbol{K}_{SSMPC} = \begin{bmatrix} \boldsymbol{I}_p & \boldsymbol{0}_{p\times p(M-1)} \end{bmatrix} \left(\boldsymbol{G}^T\bar{\boldsymbol{Q}}\boldsymbol{G} + \bar{\boldsymbol{R}}\right)^{-1} \boldsymbol{G}^T\bar{\boldsymbol{Q}} \tag{12}$$

7. Let $k = 0$, $\boldsymbol{x}(-1) = \boldsymbol{0}$ and $\boldsymbol{u}(-1) = \boldsymbol{0}$.

Main Routine

1. Read the process state vector $\boldsymbol{x}(k)$ and the reference $\boldsymbol{y}_{ref}(k)$.
2. Determine $\boldsymbol{y}(k) = \boldsymbol{Cx}(k)$.
3. Determine $\boldsymbol{\Delta x}(k) = \boldsymbol{x}(k) - \boldsymbol{x}(k-1)$.
4. Assemble the extend state vector as:

$$\tilde{\boldsymbol{x}}(k) = \begin{bmatrix} \boldsymbol{\Delta x}(k) \\ \boldsymbol{y}(k) \end{bmatrix} \tag{13}$$

5. Determine the free-response vector $\boldsymbol{F} = \boldsymbol{\phi}\tilde{\boldsymbol{x}}(k)$.
6. Assemble the reference vector as $\boldsymbol{Y}_{ref} = [\boldsymbol{y}_{ref}, \boldsymbol{y}_{ref}, ..., \boldsymbol{y}_{ref}]$ (size $pN \times 1$).
7. Determine the control increment, give by

$$\boldsymbol{\Delta u}(k) = \boldsymbol{K}_{SSMPC}(\boldsymbol{Y}_{ref} - \boldsymbol{F}) \tag{14}$$

8. Update the control action making $\boldsymbol{u}(k) = \boldsymbol{u}(k-1) + \boldsymbol{\Delta u}(k)$.
9. Do $k = k + 1$ and return to the first step of the main routine.

It is important to note that as a expanded model system (Eq. (9)) is used, this strategy has an integral control action (Cavalca *et al.*, 2010). Therefor this SSMPC algorithm accommodates constants disturbances.

ISSN 2176-5480

3. THREE-PHASE INDUCTION MOTOR

In order to reach a representative analytical mathematical model of a TIM, it is necessary to assume some simplification hypotheses. It is important to established a compromise between model accuracy and complexity, seeking an appropriate balance. Thus, in this paper the three stator windings, as well the rotor ones, are considered equal and equally spaced. The air gap is taken as constant and the magnetic circuit as ideal, with no saturation or magnetic losses. Still, assume a TIM with rotor windings short-circuited, thus rotor tensions are null.

It is usual to adopt a two-phase representation, in order to simplify the model, reducing the number of equations. This representation is made possible by the symmetry displayed by the system. Also, objecting to obtain a no oscillatory behavior of the some TIM variables, the two-phase axes are defined rotating. Therefore, the variables represented in such rotating two-phase coordinate system may behave continuously, depending on how the axis are rotated. The angular position of this rotating dq system, θ, commonly known as reference frame, can assume any desirable value along time. However, it is convenient to use for θ a TIM variables, as the rotor position, for example. A complete deduction of such transformations and more about TIM modeling can be found in (Novotny and Lipo, 1996) and (Krause *et al.*, 1995). Applied such transformations, the TIM model takes the form:

$$v_{ds} = R_s i_{ds} + L_s i_{ds}^{'} + L_s \omega i_{qs} + L_m i_{dr}^{'} - L_m \omega i_{qr} \tag{15}$$

$$v_{qs} = R_s i_{qs} + L_s i_{qs}^{'} + L_s \omega i_{ds} + L_m i_{qr}^{'} - L_m \omega i_{dr} \tag{16}$$

$$v_{dr} = R_r i_{dr} + L_r i_{dr}^{'} + L_r(\omega - \omega_r) i_{qr} + L_m i_{ds}^{'} - L_m(\omega - \omega_r) i_{qs} \tag{17}$$

$$v_{qr} = R_r i_{qr} + L_r i_{qr}^{'} + L_r(\omega - \omega_r) i_{dr} + L_m i_{qs}^{'} - L_m(\omega - \omega_r) i_{ds} \tag{18}$$

where ω is the two-phase coordinate system rotating velocity, q and d names the new two-phase axes, and R and L represents respectively electricals resistences and inductions of the TIM, assumed constants.

Finally, the TIM model is complete adding the electromechanical equations:

$$T_e = \frac{3}{2}\frac{n_p}{2}(i_{qs} i_{dr} + i_{ds} i_{qr}) = \frac{2J}{n_p}\omega_r^{'} + \frac{2B_m}{n_p}\omega_r + T_l \tag{19}$$

in which T_e is the electrical torque, ω_e is the rotor angular velocity, n_p is the numbers of the machine poles pairs, J_m the rotor inertial moment, B_m the viscous friction coefficient of the bearings and T_l is the load torque.

4. CASE STUDY: MPC APPLIED IN A TIM

Consider a 3 CV WEG® TIM with the following specifications:

Table 1. TIM specifications.

Data	Parameters	Value	Unit
Nominal velocity	ω_n	1710	RPM
Nominal frequency	f_e	60	Hz
Nominal line voltage	V_l	380	V
Nominal line current	I_l	4.68	A
Nominal load	T_l	12.4	$N \times m$
Number of poles pairs	n_p	2	$-$
Stator resistance by phase	R_s	2.5	Ω
Rotor resistance by phase	R_r	2.24	Ω
Stator inductance by phase	L_s	288	mH
Rotor inductance by phase	L_r	288	mH
Mutual inductance	L_m	270	mH
Viscous friction coefficient	B_m	2.7×10^{-3}	$kg \times m^2/s$
Moment of Inertia	J_m	13.5×10^{-3}	$kg \times m^2$

Such TIM was phenomenological modeling considering the nonlinear electromechanical equations, Eqs. (15)-(18) and Eq. (19), and the parameters of Tab. 1. In order to obtain a no oscillatory v_{dq} behavior, the reference frame was conveniently choose as the angular position of the phase A electrical voltage θ_e. It is possible to show that with such reference frame, the v_{qs} is null.

DMC and SSMPC approaches was evaluating by numerical simulations implemented in Scilab-Xcos®. Both nonlinear mathematical model and control loop was designed using Scilab-Xcos® C-language block (*C Block 2*) and basic math operation blocks.

It is worth noting that such numerical simulations has been emulated the continuous process, in this case the specified TIM, using a elevated sample frequency. On the other hand, the continuous process has been controlled by a sampling-time digital control using zero-order-holders (ZOH). Therefore, a discrete representation of the combination of a TIM with digital-analogical converters is needed. In this paper, a sample time of $T_{st} = 1\ ms$ is used. Such sampling choice was based on the presented studies in de Santana *et al.* (2008) which satisfactory implement an adaptive SSMPC in a digital signal processor (DSP).

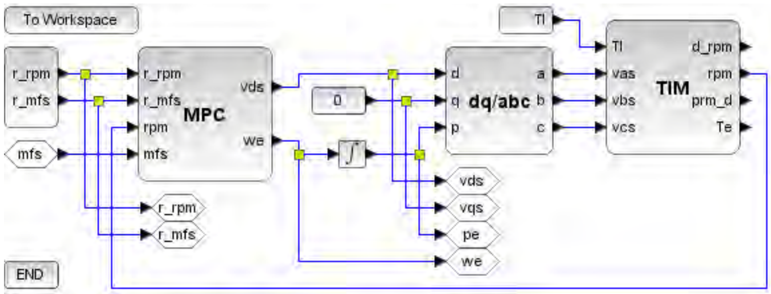

Figure 2. Environment used to emulate a TIM MPC loop.

Figure 2 shows the Scilab-Xcos® file that has been used to numerical evaluate the applicably and characteristics of a TIM MPC loop. As can be seen, there are two main blocks, TIM and MPC, which implement the TIM nonlinear dynamics and perform a MPC loop, respectively. Still, a conversion block (dq/abc) is needed to convert the dq-signals to abc-signals. It was assumed that the information of the rotor velocity and stator flux magnitude are available for feedback.

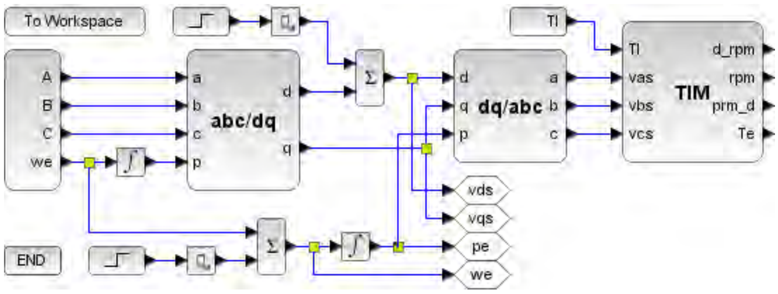

Figure 3. Environment used to obtain the TIM step response.

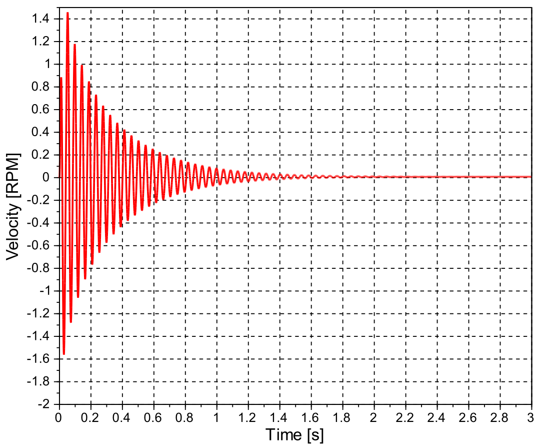

Figure 4. Step response from v_{ds} to ω_r.

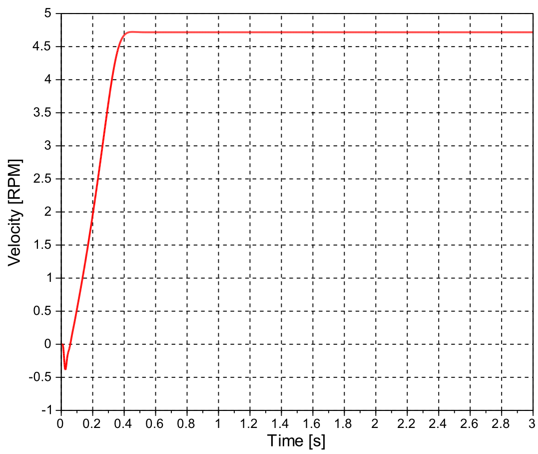

Figure 5. Step response from ω_e to ω_r.

4.1 Linear discrete-time modeling

The proposed MPC approaches, DMC and SSMPC, require a linear discrete-time mathematical model of the process. In this case, the process is nonlinear one. As consequence, a system identification method based on the step response of

ISSN 2176-5480

the classical non-linear TIM model was performed in a certain operational point.

4.1.1 Step response model

As previously states in Section 2.1, in the preliminary steps of DMC algorithm has been necessary to obtain the system step response $\boldsymbol{g}_{ij}(n), n = 1, ..., N_s$ for the variation of input u_i $(i = 1, \ldots, p)$ in the output y_j $(j = 1, \ldots, q)$, both from a defined operational point.

At this context, two-phase TIM model has two manipulated inputs $(p = 2)$, v_{ds} and the variation rate of the reference frame $\omega_e = \theta_e^{'}$. As the objective of this paper is to evaluates a rotor velocity control, the outputs has been chosen as the velocity itself, ω_r, and magnitude of the stator flux $|\lambda_s|$. The last one, has been selected to preserve the energy efficiency transfer of the magnetic circuit. Therefore, $q = 2$.

Figure 3 shows the simulation structure used to obtain the step response model. In consequence of the TIM dynamics characteristics, a single step in a isolated input, keeping the other one null, does not implicate in a output value change. As results, the step response model must to be obtained from an operational point. In this context, a three-phase voltage source mathematical representation is used to conduce TIM to such arbitrary point. Finally, a pair of conversion blocks allow to introduce the needed steps in the control signals.

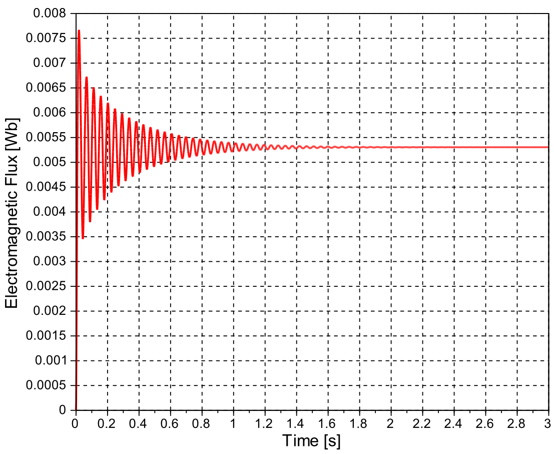

Figure 6. Step response from v_{ds} to $|\lambda_s|$.

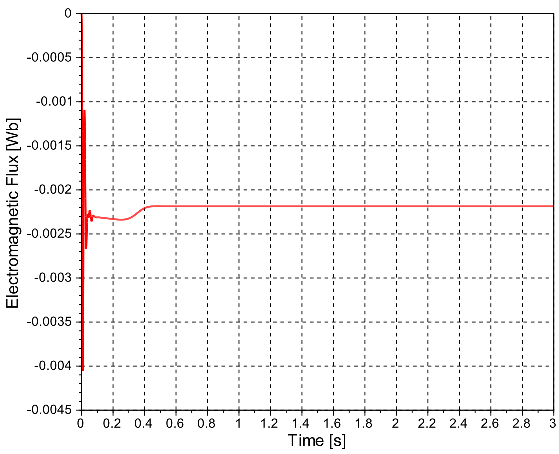

Figure 7. Step response from ω_e to $|\lambda_s|$.

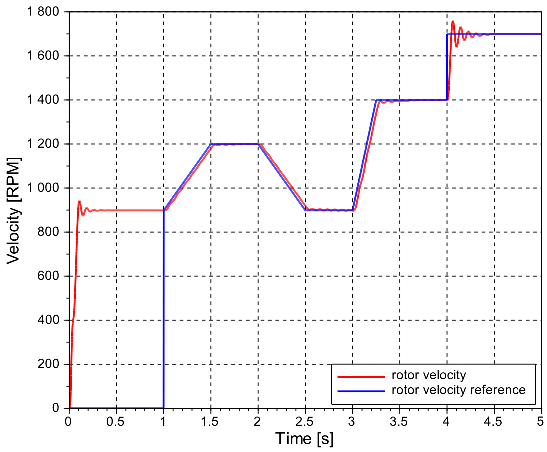

Figure 8. DMC response: ω_r.

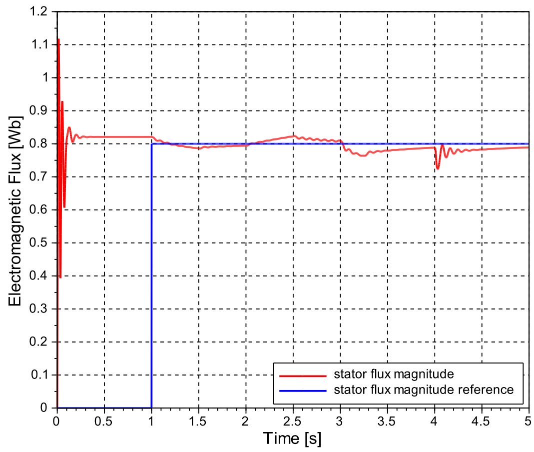

Figure 9. DMC response: $|\lambda_s|$.

The operational point, $(\omega_r)_{op}$ and $|\lambda_s|_{op}$, was arbitrary chosen as the stead state values of ω_r and $|\lambda_s|$ when $v_{ds} = \sqrt{2/3}V_l/2$ and $\omega_e = 2\pi f_e/2$ is applied.

Figures 4, 5, 6 and 7 show ω_r and $\lambda_s|$ sampled normalized variations for input steps around the operational point. Such collection of curves compose a discrete-time linearized MIMO TIM model. Such data histories compose $\boldsymbol{g}_{ij}(n), n = 1, ..., N_s$ with $N_s = 3000$.

4.1.2 State-space model

Using a Scilab® system identification function, *time_id()*, with a first-order regression, a linearized discrete-time representation for $T_{st} = 1\ ms$, can be obtained as:

$$\underbrace{\begin{bmatrix} \omega_r(k+1) \\ |\lambda_s|(k+1) \\ \omega_r(k) \\ |\lambda_s|(k) \\ v_{ds}(k) \\ \omega_e(k) \end{bmatrix}}_{\boldsymbol{x}(k+1)} = \underbrace{\begin{bmatrix} 1.9871 & 0 & -0.9872 & 0 & -0.0001 & -0.0133 \\ 0 & 1.8505 & 0 & -0.8552 & -0.0002 & 0.0002 \\ 1 & 0 & 0 & 0 & 0 & 0 \\ 0 & 1 & 0 & 0 & 0 & 0 \\ 0 & 0 & 0 & 0 & 0 & 0 \\ 0 & 0 & 0 & 0 & 0 & 0 \end{bmatrix}}_{\boldsymbol{A}} \underbrace{\begin{bmatrix} \omega_r(k) \\ |\lambda_s|(k) \\ \omega_r(k-1) \\ |\lambda_s|(k-1) \\ v_{ds}(k-1) \\ \omega_e(k-1) \end{bmatrix}}_{\boldsymbol{x}(k)} + \underbrace{\begin{bmatrix} 0.0001 & 0.0134 \\ 0.0002 & -0.0002 \\ 0 & 0 \\ 0 & 0 \\ 1 & 0 \\ 0 & 1 \end{bmatrix}}_{\boldsymbol{B}} \underbrace{\begin{bmatrix} v_{ds}(k) \\ \omega_e(k) \end{bmatrix}}_{\boldsymbol{u}(k)} \quad (20)$$

$$\underbrace{\begin{bmatrix} \omega_r(k) \\ |\lambda_s|(k) \end{bmatrix}}_{\boldsymbol{y}(k)} = \underbrace{\begin{bmatrix} 1 & 0 & 0 & 0 & 0 & 0 \\ 0 & 1 & 0 & 0 & 0 & 0 \end{bmatrix}}_{\boldsymbol{C}} \boldsymbol{x}(k) \quad (21)$$

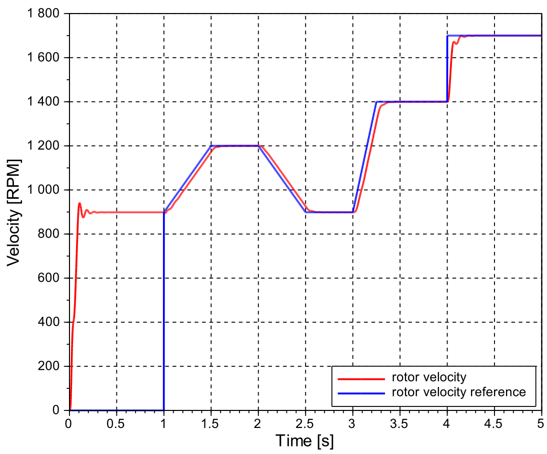

Figure 10. SSMPC response: ω_r.

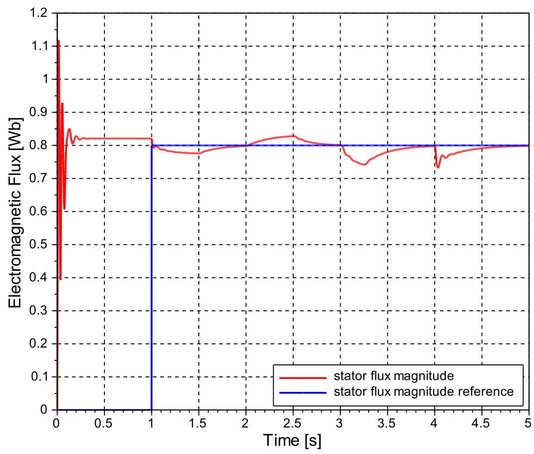

Figure 11. SSMPC response: $|\lambda_s|$.

4.2 DMC

Consider DMC algorithm presented in Section 2.1 and the step response $\boldsymbol{g}_{ij}(n)$, with $n = 1, \ldots, N_s$, $i = 1, \ldots, p$ and $j = 1, \ldots, q$, from Section 4.1.1. The simulation structure is shown in Fig. 2 and control parameters are set in $N = 5$, $M = 2$, $\mu_1 = 100$, $\mu_2 = 0.4$, $\rho_1 = 1$ and $\rho_2 = 100$. Such parameters adjusting are based on evaluating numerical simulations in order to determined the main influences of each control parameter. In this case, lower values of N and M results in a more adequate behavior as well as in a reduction of the computacional cost. Similar fact has been verified in de Santana *et al.* (2008). The accuracy of the prediction model can explain such fact. In this case, it is interesting using a more conservative control law, which is typically active by chosen lower value of the horizons and bigger values of the weight control effort $\boldsymbol{\mu}$. Figures 8-13 show the simulation results for the proposed TIM DMC loop.

In the first second of simulation the TIM is taken to the operational point. After that, the control algorithm is started and an increasing velocity reference ramp is imposed, from the operational point in $t = 1\ s$ to 1200 RPM in $t = 1,5$

ISSN 2176-5480

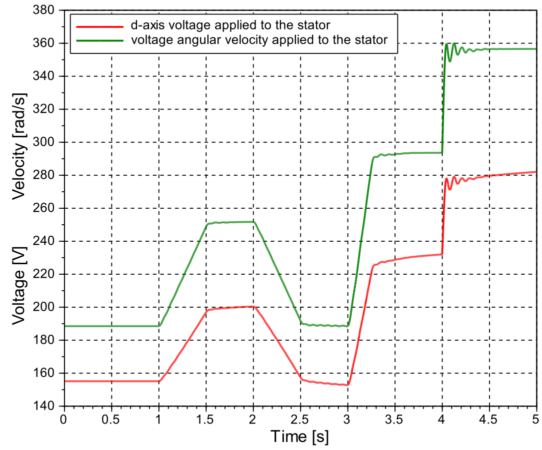

Figure 12. DMC response: v_{ds} and ω_e.

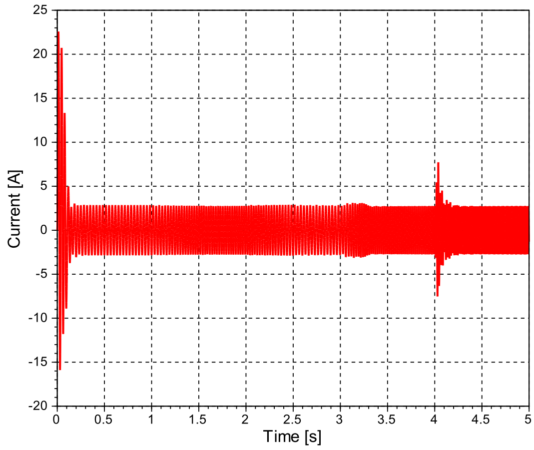

Figure 13. DMC response: i_{as}.

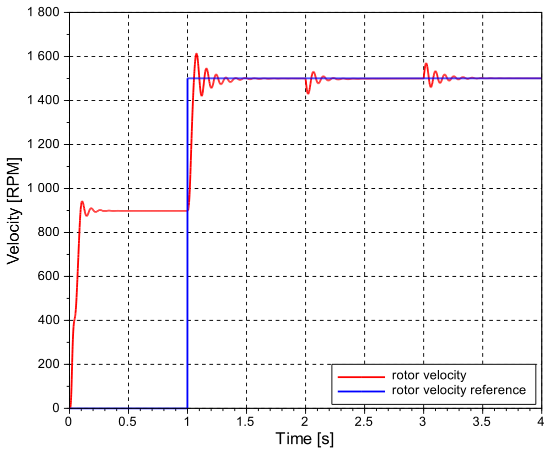

Figure 14. DMC load response: ω_r.

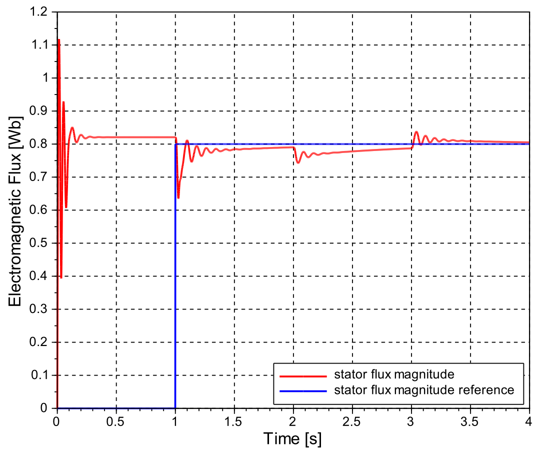

Figure 15. DMC load response: $|\lambda_s|$.

s. Therefore, an similar decrease velocity ramp reference is introduced in order to return the system to the operational point. Finaly, a more abrupt velocity reference ramp and a step velocity reference are applied, in $t = 3$ s and $t = 4$ s, respectively. Figures 8 and 9 present the output variables responses. As can be seen, both converge to the reference. Moreover, Fig. 12 and 13 show the applied control actions, v_{ds} and ω_e, and the stator A-phase current, respectively. All those variables respect the physical constraints and expected energy spend.

Figures 14, 15 and 16 show input and output variables, respectively, in case of the nominal load adding ($t = 2$ s) and withdrawal ($t = 3$ s). As expected, the control loop was able to accommodate such constant disturbance. Still, Fig. 17 show the stator A-phase current, which has an adequate behavior.

4.3 SSMPC

Consider SSMPC algorithm presented in Section 2.2 and the state space Eq. (21) and (21). Again, consider the simulation structure shown in Fig. 2, but with the control parameters setting in $N = 5$, $M = 2$, $\mu_1 = 0.4$, $\mu_2 = 40$, $\rho_1 = 1$ and $\rho_2 = 150$. Figures 10-19 show the analogous DMC simulation results for the SSMPC algorithm. Figures 10 and 11 present the output variables responses, which again converge to the reference. Moreover, Fig. 18 and 19 show the applied control actions, v_{ds} and ω_e, and the stator A-phase current, respectively. Finally, Fig. 20 and 21 and Fig. 22 show input and output variables, respectively, in case of the nominal load adding ($t = 2$ s) and withdrawal ($t = 3$ s). Due to the integral control action, the control loop was able to accomodate such disturbance. Finally, Fig. 23 shows the behavior of stator A-phase current, which is adequate for such load condition.

ISSN 2176-5480

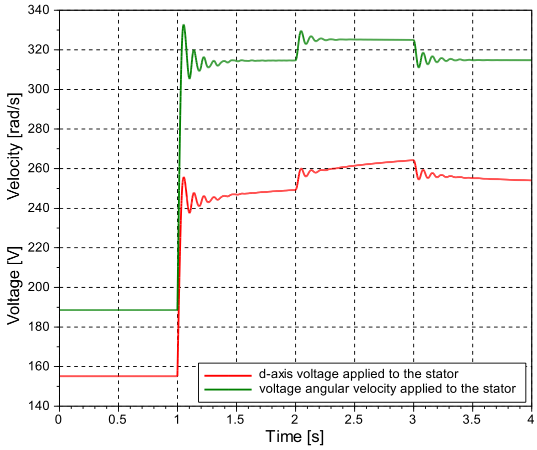

Figure 16. DMC load response: v_{ds} and ω_e.

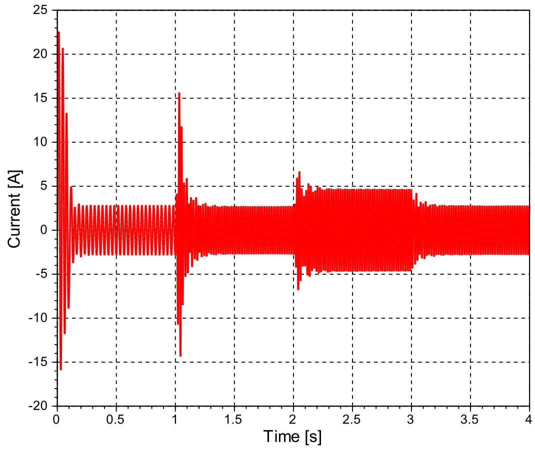

Figure 17. DMC load response: i_{as}.

4.4 COMPARATIVE CONSIDERATIONS

All the simulations were performed on a computer with Intel® i5-2450M@2.5GHz processor and 6GB RAM, running Windows® 7 Professional and Scilab® 5.4.1. The computation average time required to obtain the simulation results in Fig. 8 were 1.6175 seconds, for the DMC control approach. Already for the SSMPC approach, represented in Fig. 10, the simulation has been taken 0.3562 seconds.

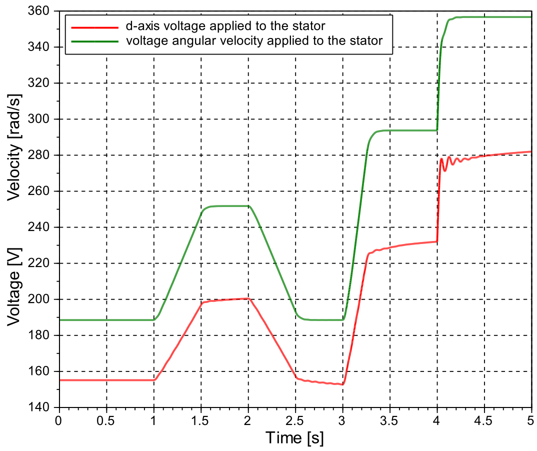

Figure 18. SSMPC response: v_{ds} and ω_e.

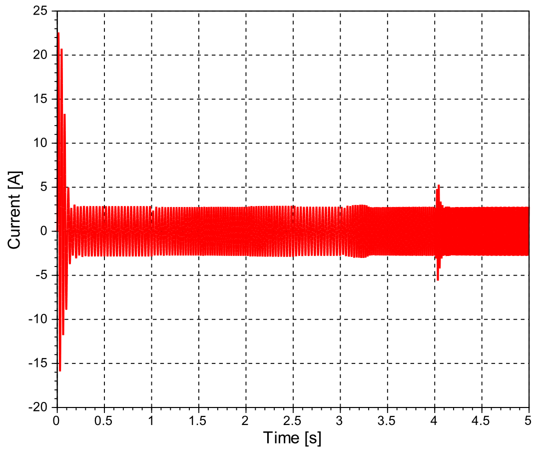

Figure 19. SSMPC response: stator A-phase current i_{as}.

In one hand, DMC has a simpler and faster way to obtain the prediction model, however, by other side, such formulation requires a high computational cost. In SSMPC, using a state space model, the required simulation time decreases significantly. However, as result of the first order approximation used in this paper and the control parameters adjusting, the SSMPC loop presents more conservative results.

5. CONCLUDING REMARKS

The applicability of DMC and SSMPC techniques were evaluated in a TIM speed control loop. The control algorithms, as well as the nonlinear mathematical model of the motor, were programmed using the free computing environment Scilab-Xcos®. Simulation results, with variations in load and speed reference, demonstrates that is possible to aply MPC approachs with a good performance.

In future work, a phenomenological state space modeling will be considered in order to improve the control loop behavior. In this sense, adaptive methods stand out as a good solution (de Santana *et al.*, 2008), since a TIM is a extremely non-linear system.

ISSN 2176-5480

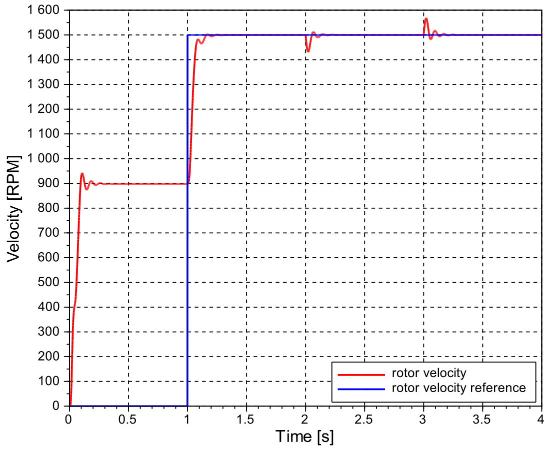

Figure 20. SSMPC load response: ω_r.

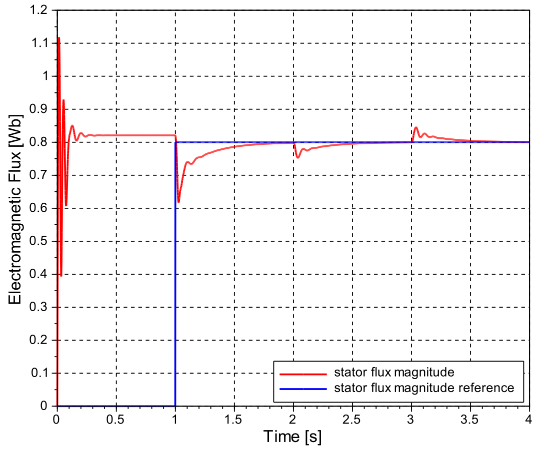

Figure 21. SSMPC load response: $|\lambda_s|$.

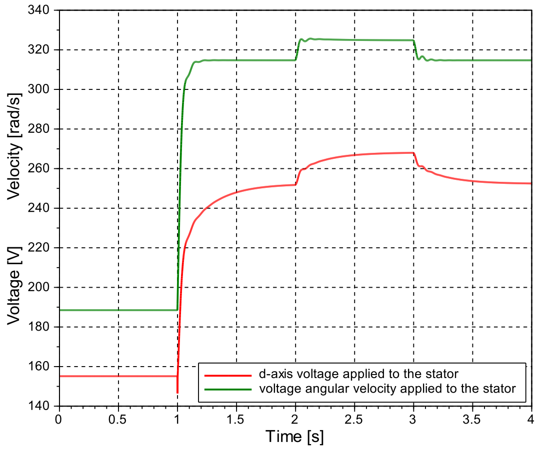

Figure 22. SSMPC load response: v_{ds} and ω_e.

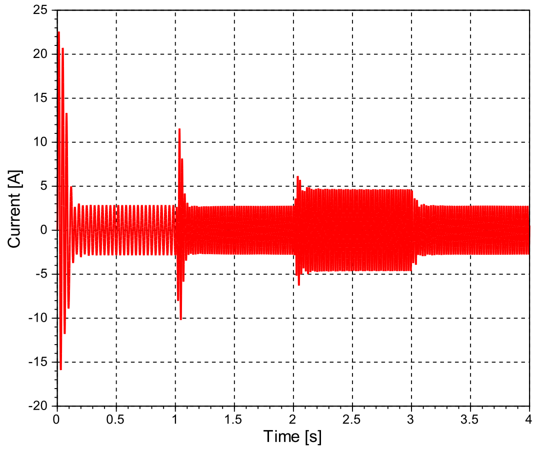

Figure 23. SSMPC load response: i_{as}.

6. ACKNOWLEDGEMENTS

The authors gratefully acknowledge the support of the National Counsel of Technological and Scientific Development - CNPq and of the Coordination of Higher Education Personnel Improvement - CAPES - Brazil (research fellowships).

7. REFERENCES

Camacho, E.F. and Bordons, C., 1999. *Model Predictive Control*. Spring-Verlag, London, UK.

Cavalca, M.S.M., Galvão, R.K.H. and Yoneyama, T., 2010. "Integrator resetting with guaranteed feasibility for an LMI-based robust model predictive control approach". In *Proceedings of the 18th Mediterranean Conference on Control and Automation*. Marrakech, Morocco, 2010.

de Santana, E.S., Bim, E. and C., A.W., 2008. "Algoritmo preditivo baseado em modelo aplicado ao controle de velocidade do motor de indução". *Revista Controle & Automaćão*, Vol. 19, No. 2, pp. 156 – 164.

Krause, P.C., Wasynczuk, O. and Sudhoff, S.D., 1995. *Analysis of electric machinery*. IEEE Press, New York, EUA.

Lee, J.H., 2011. "Model predictive control: Review of the three decades of development". *International Journal of Control, Automation, and Systems*, pp. 415–424.

Maciejowski, J.M., 2002. *Predictive Control with Constraints*. Prentice Hall, Harlow, England.

Novotny, D.W. and Lipo, T.A., 1996. *Vector control and dynamics of AC drives*. Oxford University Press, New York, EUA.

Qin, S.J. and Badgwell, T.A., 2003. "A survey of industrial model predictive control technology". *Control Engineering*

Practice, Vol. 11, pp. 733–764.
Rossiter, J.A., 2004. *Model-Based Predictive Control.* CRC Press LLC, New York, USA.

8. RESPONSIBILITY NOTICE

The authors are the only responsible for the printed material included in this paper.